This is an *Accepted Manuscript*, which has been through the Royal Society of Chemistry peer review process and has been accepted for publication.

Accepted Manuscripts are published online shortly after acceptance, before technical editing, formatting and proof reading. Using this free service, authors can make their results available to the community, in citable form, before we publish the edited article. We will replace this *Accepted Manuscript* with the edited and formatted *Advance Article* as soon as it is available.

You can find more information about *Accepted Manuscripts* in the **Information for Authors**.

ChemComm

Dynamic Article Links ▶

COMMUNICATION

A polyimide anode with high capacity and superior cyclability for aqueous Na-ion batteries

Wenwen Deng, Yifei Shen, Jiangfeng Qian, and Hanxi Yang*

A redox-active and water-insoluble polyimide, poly-(naphthalene four formyl ethylenediamine), demonstrates a high capacity of 130 mAh g^{-1}, a strong rate capability at 10 C rate and an excellent capacity retention of 91.2% over 1000
10 **cycles, offering a low cost and environmentally benign anode for aqueous Na-ion batteries.**

Aqueous Na-ion batteries have recently attracted considerable interest for electric energy storage applications because of their low cost and intrinsic safety.[1,2] In the development of this new
15 technology, a number of host materials such as Mn-based oxides[3-5] and Prussian blue type $Na_xM_yFe(CN)_6$ (M =Ni, Cu, etc.)[6,7] have been revealed to have considerable cyalability in aqueous electrolytes; however, only a few of anode materials have been reported for aqueous Na-ion batteries, possibly due to the narrow
20 electrochemical window of water.[8] Recently, S. Park et al. introduced a NASICON-type $NaTi_2(PO_4)_3$ as aqueous anode for Na-ion batteries,[9] which showed a quite low voltage of -0.8V with a reversible capacity of ~140 mAh g^{-1}. Later, Y. Cui et al.[10] demonstrated an open-frame structured hexacyanomanganate
25 (Mn(CN)Mn) anode[11] with excellent rate capability and cycling stability. Despite of their adequate anodic performances, these materials are all based on transitional metals that may impose severe cost and resource restrictions for widespread applications. Organic materials seem to be a good candidate for aqueous Na-
30 storage anodes because of their abundance, environmental friendliness and structural diversity.[11] In recent years, a variety of organic molecules[12,13] and polymers[14-17] have been explored as Li- or Na- host materials, but most of these materials can only deliver their redox capacities in organic electrolytes and fail to
35 work in aqueous solutions. Though a few of redox-active polymers such as poly-(2-vinylanthraquinone),[18] polypyrrole[19] and polyimides[20] were investigated as aqueous anodes, they are not paid enough attention to their Na-storage properties. Up to now, development of an organic aqueous Na-storage anode still
40 remains a challenge for the battery chemistry.

In the search for Na-storable organic materials, we focused on polyimides and tried to improve their Na-insertion performance by tailoring the aromatic moieties in the polymer chains. By electrochemical evaluation of different aromatic carbonyl
45 derivatives, we found that some of the polyimides such as poly-(naphthalene four formyl ethylenediamine) (PNFE) can undergo were reversible redox reaction along with Na$^+$ insertion/extraction in aqueous solution at quite low potential (-0.50 V vs. Ag/AgCl).

In this paper, we reported the Na-storage behaviour of PNFE with
50 emphasis on its possible application as an organic anode for aqueous Na-ion batteries.

PNFE polymer was prepared by a dehydration condensation reaction according to the method previously reported.[21] To evaluate the electrochemical properties of PNFE in aqueous
55 Na_2SO_4 electrolyte, the PNFE electrode was prepared by mixing 60% PNFE powder, 30% conductive carbon and 10% polytetrafluroethylene binder by weight and then used for charge/discharge measurements. Experimental details for the electrode preparation and cell assembly of the perylenediimides
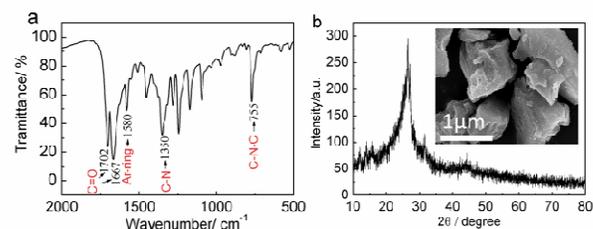60 are described in Electronic Supplementary Information (ESI).

Figure 1 a. FTIR spectrum of the as-prepared PNFE sample; **b.** XRD patterns of the PNFE and PNFE/C composite

65 The chemical structure of PNFE was confirmed by FTIR spectrometry. Figure 1a shows the FTIR spectrum of the as-prepared PNFE, which features a typical imide structure: the absorption bands at 1702 cm^{-1} and 1667 cm^{-1} correspond to the asymmetric and symmetric stretching vibrations of C=O bond,
70 respectively. The strong absorption at 1350 cm^{-1} reflects the stretching vibration of the C-N bond, whereas the absorption at 755cm^{-1} belongs to the asymmetric stretching vibration of the tertiary formamides C-N-C bond.[22] In addition, the band at 1580 cm^{-1} is characteristic of the stretching vibration of the
75 naphthalene ring. All the IR features point to a naphthalene-derived polyimide. Figure 1b gives the XRD pattern of the pristine PNFE. The PNFE sample demonstrates a broad and weak diffraction band at 2θ = 25°, suggesting that this polymer has an amorphous structure. As can be visualized in the inset of Figure
80 1b, the PNFE sample appears as aggregated particles with an average size of ~ 2 μm.
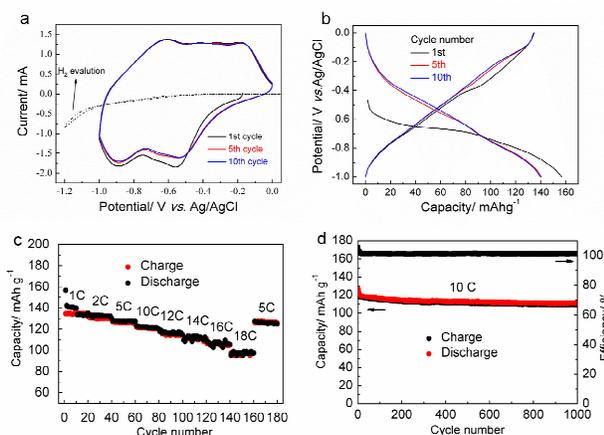
Figure 2 Electrochemical performances of the PNFE electrode: **a.** CV curves measured at a scan rate of 10 mV s^{-1}; **b.** Charge/discharge profiles in first ten cycles at a current density of 100 mA g^{-1}; **c.** Reversible capacities cycled at changing rates (1 C=100 mA g^{-1}); **d.** Long-term cycling stability at a constant current of 10 C. All the cells were cycled between -1.0 to 0 V

To reveal the electrochemical redox activity, the PNFE electrode was firstly characterized by cyclic voltammetry. As shown in Figure 2a, two reduction peaks appear at -0.55 V and -0.9 V during first cathodic scan and correspondingly there appear two oxidation peaks at -0.75 V and -0.25 V at reversed anodic scan, implying a reversible two-electron redox reaction in the polymer chains. During subsequent cycles, these two pairs of redox peaks remained almost unchanged in their intensities and shapes, demonstrating an excellent electrochemical reversibility and cycling stability of the polymer structure. According to previous studies of the redox mechanism of aromatic imides,[19] the CV peaks of the PNFE compound can only be assigned to the electrochemical enolization reaction of the carbonyl groups in the polyimide structure evolving a two-electron redox reaction along with 2 Na$^+$ ions associating with and disassociating from the oxygen atoms of the imide groups. This redox process can be regarded as a Na$^+$-storage reaction as shown in Scheme 1:
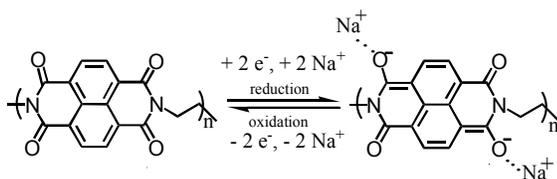
Scheme 1 The reaction mechanism of PNFE electrode

The charge/discharge performance of the PNFE material was examined as an organic anode in 1M Na$_2$SO$_4$ solution. As given in Figure 2b, the charge/discharge capacities of PNFE at the first cycle are 156.84/134.4 mAh g^{-1} respectively, corresponding to a high initial columbic efficiency of 83.6%. Since the second cycle, the charge/discharge efficiency rapidly rose up to ~95% and the reversible capacity kept stable at 134 mAh g^{-1}. Particularly, the average charge/discharge potentials of the polymer locate at a quite low region of -0.50 V, suitably serving as a high capacity anode for aqueous Na-ion batteries. In addition to its high reversible capacity, the PNFE anode also exhibits a high-rate capability and long-term cyclability. Figure 2c shows the

reversible capacities of the PNFE electrode at changing rates. When the current rate was increased from 1 C to 12 C (1C = 100 mAh g^{-1}), the reversible capacity of the PNFE electrode decreased slightly from 134 mAh g^{-1} to 112 mAh g^{-1}. Even at a very high rate of 18 C (1.8 A g^{-1}), the electrode can still deliver a reversible capacity of ~95 mAh g^{-1}, demonstrating a strong rate performance in the aqueous electrolyte. As displayed in Figure 2d, the PNFE electrode also exhibits a remarkable cyclability at high rate of 10C with almost no discernible capacity decay after 1000 cycles. This cycling stability at a high-rate is hardly seen from other organic cathodes, probably due to the high activity of the carbonyl groups on the flexible skeleton, which allow fast Na$^+$ transportation in the polyimide chains for the redox reaction. Also, the chemically stable and water-insoluble PNFE chains enable a long cycle life in aqueous electrolytes.
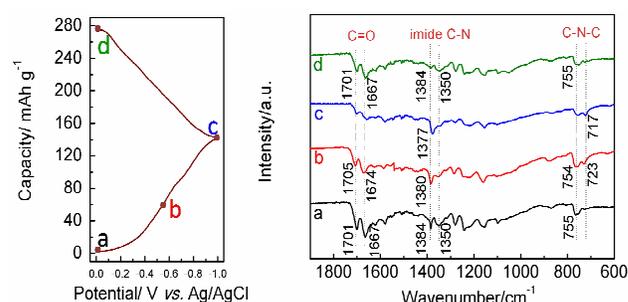

Figure 3 IR spectra (right) of the PNFE anode recorded at the different potentials as indicated in the charge and discharge curve (left)

To gain insight into the redox mechanism of the PNFE, the changes in the bonding states of the PNFE backbones at different depths of charge and discharge were characterized by FTIR analysis. As shown in Figure 3, the vibrational modes of the C=O, C-N and C-N-C groups of the polyimide vary considerably during charge and discharge. When firstly discharged to -0.55 V, the peak intensities of the C=O bond decreased noticeably and shifted from 1667 and 1701 cm^{-1} to a higher wavenumbers 1705 and 1674 cm^{-1}, suggesting an electron injection into the C=O bond for reduction reaction. Meanwhile, the absorptions of the C-N bonds at 1350 cm^{-1} at 1384cm^{-1} become weaker and slightly shifted to lower wavenumbers due to the weakening of the C-N bonds along with the reduction of C=O groups. When further discharged to -1.0 V, the C=O absorptions were almost indiscernible, reflecting that most of the C=O groups were reduced to an enol structure. Certainly, this reduction reaction must involve Na$^+$- insertion into the polymer chains and then bonding to the C=O groups. In the reversed charge to 0 V, the absorption bands of the C=O, C-N and C-N-C groups recovered fully their original positions and intensities, implying a reversible rearrangement of the C=O bonds with simultaneous remove of Na$^+$ ions from the PNFE chains during charge reaction.

To further confirm the Na$^+$ insertion–extraction mechanism, quantitative ICP analysis of the Na+ content cycled in the PNFE electrode were performed at different depths of charge and discharge (see ESI table 1). At first discharge to -0.55 V, the Na content in the PNFE anode is calibrated to be 7.38 %, corresponding to 0.94 Na$^+$ in one PNFE unit. Once fully discharged to -1.0 V, the Na content stored in the polymer anode

is measured to be 16.24 %, corresponding to 2 Na$^+$ ions bound in each PNFE unit (Scheme 1). At the reversed charge to 0 V, almost no discernible amount of Na$^+$ ions can be detected in the electrode, confirming the complete removal of Na$^+$ ions from the polymer anode after full discharge.

Based on the PNFE anode, we assembled a coin type all-organic Na-ion cell using poly(2,2,6,6-tetramethylpiperidinyloxy-4-yl vinylether) (PTVE) cathode and aqueous Na$_2$SO$_4$ electrolyte. Figure S1 gives the charge-discharge curves and cycling performance of this all-organic Na-ion battery. As shown in the figure, this cell gives a high open circuit voltage of 1.75 V and delivers a reversible capacity of 75 mAh g^{-1} in terms of cathode capacity. Nevertheless, this cell can be well cycled at a high rate of 2C (1C=100 mA g^{-1}) with 85% capacity retention over 100 cycles, suggesting a possible application of the PNFE polymer as an organic anode for constructing all-organic aqueous Na-ion batteries.

In summary, we synthesized and investigated a PNFE polymer as an organic anode for aqueous Na-ion batteries. The electrochemical characterization revealed that the polymer can undergo an electrochemical enolization reaction through a reversible Na$^+$-association/disassociation with the carbonyl groups of the polymer, delivering a high capacity of 130 mAh g^{-1} at suitable anodic working potentials. In addition, this polymer anode also demonstrates a high rate capability and excellent cyclability, enabling to be used for battery applications. Most significantly, this polymer material is low cost, easy to prepare and environmentally friendly, offering an attractive alternative to conventional transition-metal based anodes for developing aqueous Na-ion batteries.

Notes and references

College of Chemistry and Molecular Science, Wuhan University, Wuhan 430072, China. E-mail: hxyang@whu.edu.cn; Fax: (+) 86-27-68754526; Tel: (+) 86-27-68754526.

† Electronic Supplementary Information (ESI) available: Experimental details, ICP characterization of the cycled PNFE electrodes, charge-discharge curves and cycling performance of all-organic Na-ion battery. See DOI: 10.1039/b000000x/

1   V. Palomares, P. Serras, I. Villaluenga, K. B. Hueso, J. Carretero-González and T. Rojo, Energy & Environmental Science, 2012, 5, 5884.
2   Y. Lu, J. B. Goodenough and Y. Kim, Journal of the American Chemical Society, 2011, 133, 5756.
3   Z. Li, D. Young, K. Xiang, W. C. Carter and Y. M. Chiang, Advanced Energy Materials, 2013, 3, 290.
4   Q. Qu, Y. Shi, S. Tian, Y. Chen, Y. Wu and R. Holze, Journal of Power Sources, 2009, 194, 1222.
5   J. Whitacre, A. Tevar and S. Sharma, Electrochemistry Communications, 2010, 12, 463.
6   X. Wu, Y. Cao, X. Ai, J. Qian and H. Yang, Electrochemistry Communications, 2013, 31, 145.
7   X. Wu, M. Sun, Y. Shen, J. Qian, Y. Cao, X. Ai and H. Yang, ChemSusChem, 2014, 7, 407.
8   F. Beck and P. Rüetschi, Electrochimica Acta, 2000, 45, 2467.
9   S. I. Park, I. Gocheva, S. Okada and J.-i. Yamaki, Journal of The Electrochemical Society, 2011, 158, A1067.
10 M. Pasta, C. D. Wessells, N. Liu, J. Nelson, M. T. McDowell, R. A. Huggins, M. F. Toney and Y. Cui, Nature communications, 2014, 5.
11 Z. Song and H. Zhou, Energy & Environmental Science, 2013, 6, 2280.
12 L. Zhao, J. Zhao, Y. S. Hu, H. Li, Z. Zhou, M. Armand and L. Chen, Advanced Energy Materials, 2012, 2, 962.
13 R. Zhao, Y. Cao, X. Ai and H. Yang, Journal of Electroanalytical Chemistry, 2013, 688, 93.
14 L. Zhu, A. Lei, Y. Cao, X. A and H. Yang, Chemical communications, 2013, 49, 567.
15 W. Deng, X. Liang, X. Wu, J. Qian, Y. Cao, X. Ai, J. Feng and H. Yang, Scientific reports, 2013, 3.
16 L. Zhu, Y. Shen, M. Sun, J. Qian, Y. Cao, X. Ai, H. Yang, Chemical communications, 2013, 49, 11370
17 Y. Shen, D. Yuan, X. Ai, H. Yang and M. Zhou, Electrochemistry Communications, 2014, 49, 5.
18 W. Choi, D. Harada, K. Oyaizu and H. Nishide, Journal of the American Chemical Society, 2011, 133, 19839.
19 M. Pasta, C. D. Wessells, R. A. Huggins and Y. Cui, Nature communications, 2012, 3, 1149.
20 H. Qin, Z. Song, H. Zhan and Y. Zhou, Journal of Power Sources, 2014, 249, 367.
21 Z. Song, H. Zhan and Y. Zhou, Angewandte Chemie, 2010, 122, 8622.
22 G. Socrates, Infrared and Raman characteristic group frequencies: tables and charts, John Wiley & Sons, 2004.